Article

Continuous Spinning of a Single-Walled Carbon Nanotube–Nylon Composite Fiber

Junbo Gao, Mikhail E. Itkis, Aiping Yu, Elena Bekyarova, Bin Zhao, and Robert C. Haddon

J. Am. Chem. Soc., **2005**, 127 (11), 3847-3854• DOI: 10.1021/ja0446193 • Publication Date (Web): 22 February 2005

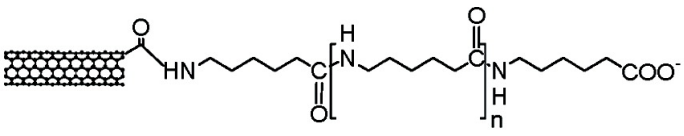

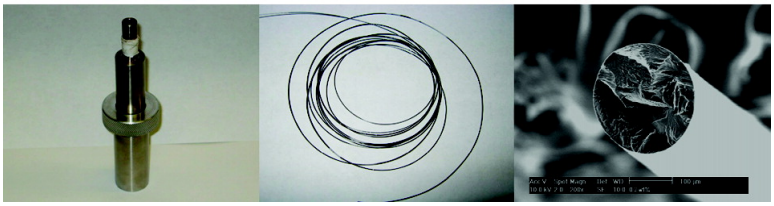

J|A|C|S
ARTICLES
Published on Web 02/22/2005

Continuous Spinning of a Single-Walled Carbon Nanotube−Nylon Composite Fiber

Junbo Gao,[†] Mikhail E. Itkis,[†,‡] Aiping Yu,[‡] Elena Bekyarova,[‡] Bin Zhao,[‡] and Robert C. Haddon*[,‡]

Center for Nanoscale Science and Engineering, Departments of Chemistry and Chemical & Environmental Engineering, University of California, Riverside, California 92521-0403 and Carbon Solutions, Incorporated, Riverside, California 92506

Received September 5, 2004; E-mail: haddon@ucr.edu

Abstract: We report a chemical processing technology that allows the continuous spinning of single-walled carbon nanotubes (SWNTs)−nylon 6 (PA6) fibers by the in-situ polymerization of caprolactam in the presence of SWNTs, which simultaneously optimizes the morphology of the composite. We show that caprolactam is an excellent solvent for carboxylic-acid-functionalized SWNTs (SWNT−COOH) and that this allows the efficient dispersal of the SWNTs and subsequent grafting of PA6 chains to the SWNTs through condensation reactions between the carboxylic-acid group on SWNT−COOH and the terminal amine group of PA6. The existence of a graft copolymer between the PA6 chains and the SWNTs is demonstrated by IR, TGA, and AFM studies, and we show that the solubility of the polymerized material in formic acid is controlled by the degree of graft copolymerization. The amount of grafted PA6 chains that are attached to the SWNTs can be adjusted by controlling the concentration of the initiator (6-aminocaproic acid). The process leads to a uniform dispersion of the SWNTs, and the presence of the graft copolymer increases the polymer/SWNT compatibility while strengthening the interfacial interaction between the nanotube and matrix. The Young's modulus, tensile strength, and thermal stability of the SWNT-reinforced composite fibers produced by this process are significantly improved.

Introduction

Fiber-reinforced polymer composites are used in many structural materials because they show a significant improvement in strength and toughness over the native polymer. To fully realize the theoretically predicted performance improvement a number of important factors must be manifested in the final composite. First, from a structural point of view, the fiber spacing should be smaller than the characteristic strength-limiting flaw,[1] and thus, smaller fiber diameters are desirable in order to produce a higher packing density. Second, a uniform fiber distribution within the matrix is necessary in order to avoid unreinforced regions in the matrix and thereby distribute the load evenly throughout the composite. To ensure efficient load transfer from the matrix to the fiber, the interfacial bonding between the polymer matrix and the fiber must be optimized to prevent fiber pull out.[2] The covalent bond between the matrix and fiber constitutes the strongest type of interfacial bonding, and it is preferred in situations where the strength of the reinforcing agent is significantly higher than that of the matrix. Carbon nanotubes are considered to be the ideal reinforcing agent for high-strength polymer composites because of their tremendous mechanical strength, nanometer-scale diameter, and high aspect ratio.[3] Studies have shown that carbon nanotubes have a ca. 1000 GPa Young's modulus which is much higher than that of conventional carbon fibers (200−800 GPa).[4−6] In the past decade a number of methods have been applied for the synthesis of carbon nanotube−polymer composites: physical mixing of the carbon nanotubes with preformed polymers in solution or in the molten state,[7−13] electrospinning,[14] in-situ polymerization in the presence of single-walled carbon nanotubes (SWNTs),[15−17] surfactant-assisted processing of SWNT−

[†] Carbon Solutions, Inc.
[‡] University of California, Riverside.

(1) Chawla, K. K. *Composite Materials Science and Engineering*; Springer-Verlag: New York, 1987.
(2) Peebles, L. H. *Carbon Fibers: Formation, Structure and Properties*; CRC Press: Boca Raton, Fl, 1995.
(3) Calvert, P. *Nature* **1999**, *399*, 210−211.
(4) Overney, G.; Zhong, W.; Tomanek, D. *Z. Phys. D, At., Mol. Clusters* **1993**, *27*, 93−96.
(5) Salvetat, J. P.; Briggs, G. A. D.; Bonard, J. M.; Basca, R. R.; Kulik, A. J.; Stockli, T.; Burnham, N. A.; Forro, L. *Phys. Rev. Lett.* **1999**, *82*, 944−947.
(6) Yu, M. F.; Files, B. S.; Arepalli, S.; Ruoff, R. S. *Phys. Rev. Lett.* **2000**, *84*, 5552−5555.
(7) Qian, D.; Dickey, E. C.; Andrews, R.; Rantell, T. *Appl. Phys. Lett.* **2000**, *76*, 2868−2870.
(8) Andrews, R.; Jacques, D.; Rao, A. M.; Rantell, T.; Derbyshire, F.; Chen, Y.; Chen, J.; Haddon, R. C. *Appl. Phys. Lett.* **1999**, *75*, 1329−1331.
(9) Ajayan, P. M.; Schadler, L. S.; Giannaris, C.; Rubio, A. *Adv. Mater.* **2000**, *12*, 750−753.
(10) Ko, F.; Gogotsi, Y.; Ali, A.; Naguib, N.; Ye, H.; Yang, G.; Li, C.; Willis, P. *Adv. Mater.* **2003**, *15*, 1161−1165.
(11) Steuerman, D. W.; Star, A.; Narizzano, R.; Choi, H.; Ries, R. S.; Nicolini, C.; Stoddart, J. F.; Heath, J. R. *J. Phys. Chem. B* **2002**, *106*, 3124−3130.
(12) Zhang, W. D.; Shen, L.; Phang, I. Y.; Liu, T. *Macromolecules* **2004**, *37*, 256−259.
(13) Meincke, O.; Kaempfer, D.; Weickmann, H.; Friedrich, C.; Vathauer, M.; Warth, H. *Polymer* **2004**, *45*, 739−748.
(14) Sen, R.; Zhao, B.; Perea, D. E.; Itkis, M. E.; Hu, H.; Love, J.; Bekyarova, E.; Haddon, R. C. *Nano Lett.* **2004**, *4*, 459−464.
(15) Park, C.; Ounaies, Z.; Watson, K. A.; Crooks, R. E.; Smith, J. J.; Lowther, S. E.; Connell, J. W.; Siochi, E. J.; Harrison, J. S.; St. Clair, T. L. *Chem. Phys. Lett.* **2002**, *364*, 303−308.

polymer composites,[18−22] and chemical modification of the incorporated carbon nanotubes.[23−27]

As a result of these studies impressive progress has been demonstrated; for example, the direct mixing of multiwalled carbon nanotubes (MWNTs) and polystyrene led to a 36−42% increase in elastic stiffness and a 25% increase in tensile strength with the incorporation of only 1 wt % of MWNTs into the polystyrene matrix.[7] In-situ polymerization of poly(*p*-phenylene benzobisoxazole) (PBO) in the presence of 10 wt % SWNTs led to a 50% increase in tensile strength together with a reduction of shrinkage and high-temperature creep.[16] By using surfactant-assisted dispersion of SWNTs it was possible to spin fibers from a nanotube−polymer dispersion,[21] which gave rise to fibers of low elastic modulus but exceptionally high flexibility.[5] In the case of functionalized SWNT precursors it was shown that the incorporation of 1 wt % fluorinated and acid-treated SWNTs into an epoxy composite led to a 30% increase in Young's modulus and an 18% increase in tensile strength.[23]

Thus, it is clear that the incorporation of carbon nanotubes can lead to improved performance characteristics for the polymer composites. However, the current chemical processing technologies have failed to fully realize the enormous potential of carbon nanotubes, and this has limited the performance of the materials prepared to date. In the case of direct mixing, which was employed in previous studies on MWNT−nylon 6 composites,[12,13] the high viscosity of the polymers suppresses the free movement of the carbon nanotubes in the polymer matrix during mixing and it is therefore very difficult to homogeneously disperse the nanotubes in the polymer matrix. An additional complication in the case of SWNTs is the bundled morphology which further inhibits uniform dispersion of the individual nanotubes. Furthermore, the intrinsic graphene-like atomically smooth and nonreactive surface of carbon nanotubes usually leads to a very weak interfacial interaction between the nanotubes and polymer matrix. In this situation the application of tensile stress to the composite may lead to nanotube pull out from the matrix rather than fracture,[7] and the nanotubes therefore play a limited reinforcement role. In the case of the surfactant-assisted processing method the material remaining on the surface of the nanotubes may reduce the compatibility with the host matrix.[28] Solvents are usually involved in the methods discussed above, and the evaporation of organic solvent during polymer processing increases the possibility for aggregation of the nanotubes into small domains and may result in a nonuniform dispersion of the carbon nanotubes in the final form of the polymer matrix.[29]

In the present study we demonstrate a new route to SWNT−nylon 6 composites which simultaneously optimizes SWNT dispersion and enhances the interfacial bonding through covalent grafting between the polymer chain and the engineered functionality of the SWNTs while allowing the resulting material to be spun into fibers of arbitrary length. To avoid cosolvents we used caprolactam as both a solvent and monomer for the ring-opening polymerization and graft copolymerization with the functionalized SWNTs. The covalently grafted PA6 chains alter the SWNT graphene-like chemistry, leading to a hybrid material with characteristics of both the fiber and the matrix, thereby increasing the compatibility between the SWNTs and nylon 6. Furthermore, cosolvents are avoided as a result of the excellent dispersion of the functionalized SWNTs in the amide monomer (caprolactam), and this precludes the possibility of carbon nanotube aggregation caused by solvent evaporation. The presence of PA6 chains grafted onto the SWNTs was characterized by IR, TGA, and AFM techniques, and the effect of the initiator concentration on the grafting yield was investigated. The mechanical properties and thermal stability of nylon 6−SWNTs composites were evaluated; the Young's modulus and tensile strength of the nylon 6−carbon nanotube composites in this work are significantly improved in comparison to previous work[12] involving a direct physical mixing.

Experimental Section

1. Materials and Instrumentation Purified (P3−) SWNTs were obtained from Carbon Solutions, Inc. (www.carbonsolution.com); to denote the presence of the carboxylic acid functionality, P3−SWNT material is sometimes referred to as SWNT−COOH. The P3−SWNT material is specifically tailored for functionalization chemistry; it contains ∼3−4% carboxylic acid groups as estimated by acid−base titration[30] and has a relative carbonaceous purity of 80−90%.[31] All other chemicals were purchased from Aldrich and used as received. Mid-IR spectra were measured on a Nicolet Nexus 670 FT-IR spectrometer. Atomic force microscopy (AFM) images were taken on a Digital Instruments nanoscope IIIA (using taping mode). Scanning electron microscopy (SEM) images were taken on a Philips SEM XL-30 microscope. TGA data were recorded on a Perkin-Elmer Instruments, Pyris Diamond TG/DTA Thermogravimetric/Differential Thermal Analyzer with a heating rate of 5 °C/min in air.

2. Synthesis of Nylon 6−SWNT Composites A typical synthetic procedure for the preparation of the nylon 6−SWNT composite is as follows: SWNT−COOH (44 mg) and caprolactam (8 g) were loaded into a 50 mL three-neck round-bottom flask. The mixture was sonicated at 80 °C for 2 h to produce a homogeneous SWNT dispersion. The flask was then transferred to a preheated oil bath (100 °C), and 0.8 g of 6-aminocaproic acid was added to the suspension. The suspension was heated at 250 °C with mechanical stirring under an argon atmosphere. After 6 h the product mixture was poured into water, and a very hard polymer precipitated. The precipitate was chopped into small pieces and washed with hot water at 80 °C for 1 h to remove unreacted monomer and low molecular weight oligomers.

(16) Kumar, S.; Dang, T. D.; Arnold, F. E.; Bhattacharyya, A. R.; Min, B. G.; Zhang, X.; Vaia, R. A.; Park, C.; Adams, W. W.; Hauge, R. H.; Smalley, R. E.; Ramesh, S.; Willis, P. A. *Macromolecules* **2002**, *35*, 9039−9043.
(17) Deng, J.; Ding, X.; Zhang, W.; Peng, Y.; Wang, J.; Long, X.; Li, P.; Chan, A. S. C. *Eur. Polym. J.* **2002**, *38*, 2497−2501.
(18) Vigolo, B.; Penicaud, A.; Coulon, C.; Sauder, C.; Pailler, R.; Journet, C.; Bernier, P.; Poulin, P. *Science* **2000**, *290*, 1331−1334.
(19) Barraza, H. J.; Pompeo, F.; O'Rear, E. A.; Resasco, D. E. *Nano Lett* **2002**, *2*, 797−802.
(20) Dalton, A. B.; Collins, S.; Munoz, E.; Razal, J. M.; Ebron, V. H.; Ferraris, J. P.; Coleman, J. N.; Kim, B. G.; Baughman, R. H. *Nature* **2003**, *423*, 703.
(21) Vigolo, B.; Poulin, P.; Lucas, M.; Launois, P.; Bernier, P. *Appl. Phys. Lett.* **2002**, *81*, 1210−1212.
(22) Gong, X.; Liu, J.; Baskaran, S.; Voise, R. D.; Young, J. S. *Chem. Mater.* **2000**, *12*, 1049−1052.
(23) Zhu, J.; Kim, J.; Peng, H.; Margrave, J. L.; Khabashesku, V. N.; Barrera, E. V. *Nano Lett.* **2003**, *3*, 1107−1113.
(24) Velasco-Santos, C.; Martinez-Hernandez, A. L.; Fisher, F. T.; Ruoff, R.; Castano, V. M. *Chem. Mater.* **2003**, 1049−1052.
(25) Geng, H.; Rosen, R.; Zheng, B.; Shimoda, H.; Fleming, L.; Zhou, O. *Adv. Mater.* **2002**, *14*, 1387−1390.
(26) Sano, M.; Kamino, A.; Okamura, J.; Shinkai, S. *Langmuir* **2001**, *17*, 5125−5128.
(27) Hill, D. E.; Lin, Y.; Rao, A. M.; Allard, L. F.; Sun, Y. P. *Macromolecules* **2002**, *35*, 9466−9471.
(28) Sabba, Y.; Thomas, E. L. *Macromolecules* **2004**, *37*, 4815−4820.
(29) Haggenmueller, R.; Gommans, H. H.; Rinzler, A. G.; Fischer, J. E.; Winey, K. I. *Chem. Phys. Lett.* **2000**, *330*, 219.
(30) Hu, H.; Bhowmik, P.; Zhao, B.; Hamon, M. A.; Itkis, M. E.; Haddon, R. C. *Chem. Phys. Lett.* **2001**, *345*, 25−28.
(31) Itkis, M. E.; Perea, D.; Niyogi, S.; Rickard, S.; Hamon, M.; Hu, H.; Zhao, B.; Haddon, R. C. *Nano Lett.* **2003**, *3*, 309−314.

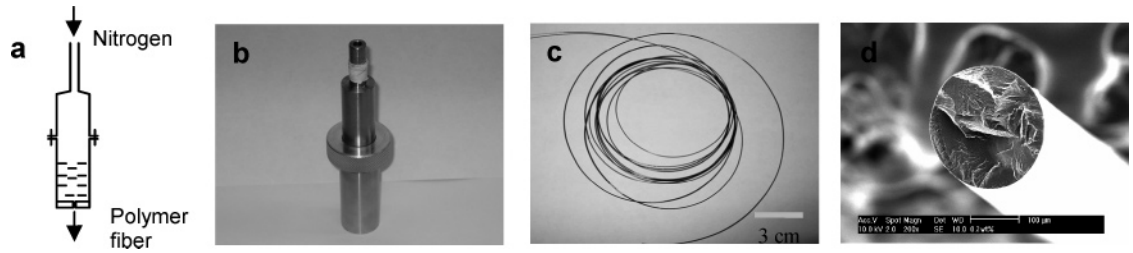

Figure 1. (a) Schematic of the fiber spinneret setup. (b) Photograph of the spinneret setup. (c) Photograph of the composite fiber. (d) SEM image of cross-sectional fracture of the composite fiber.

3. Polymer Fiber Fabrication Composite fibers were fabricated using a custom-made spinneret assembly which is illustrated in Figure 1a and b. The composite polymers were first heated at 250 °C for 20 min under the protection of a nitrogen atmosphere, and then the spinneret was pressurized with nitrogen (50 psi) to extrude the molten composite through a hole with a diameter of 400 μm. The molten composite fiber became solid as it cooled in the ambient atmosphere. The process allowed the facile fabrication of continuous black shining fibers hundreds of meters in length (Figure 1c and Supporting Information) with a smooth round surface (Figure 1d).

Results and discussion

1. Synthesis of Nylon 6−SWNTs Composites. Nylon 6−SWNTs composites with SWNT loadings between 0.1 and 1.5 wt % were synthesized by in-situ ring-opening polymerization of caprolactam in the presence of dispersed carbon nanotubes. Nitric-acid-treated SWNTs, in particular, are well dispersed in solvents containing an amide functionality such as *N*,*N*-dimethylformamide (DMF), *N*,*N*-dimethylacetamide (DMAC), and *N*-methyl-pyrrolidone (NMP).[31−36] Because caprolactam bears a strong chemical similarity to these solvents it serves as the ideal monomer for the synthesis of nylon 6. As expected, the P3−SWNTs exhibited excellent dispersion in caprolactam, and as a result of the high solubility of the carbon nanotubes in the monomer (caprolactam) and its very low viscosity, no solvents are required for the synthetic procedure reported in this study—this precludes the possibility of carbon nanotube aggregation due to solvent evaporation.

The presence of carbon nanotubes in the composite was demonstrated by Raman spectroscopy (Figure 2). The characteristic peaks at 170 and 1591 cm^{-1} correspond to the diameter-dependent radial breathing mode (RBM) and the tangential G band of the SWNTs, respectively. The disorder mode band centered at 1297 cm^{-1} which is attributed to the presence of sp^3-hybridized carbon atoms in the hexagonal framework of the carbon nanotube walls is also observed.

The composite fibers were also characterized by differential thermal analysis (DTA), and the results are shown in Figure 3. It is evident that the melting point of the composites gradually decreases as the SWNT loading in the composite is increased. The variation in the melting point of the composites as a function of the SWNT loading is presumably due to the difference in the molecular weight of the synthesized polymer, as expected based on the polymerization mechanism shown in Scheme 1.

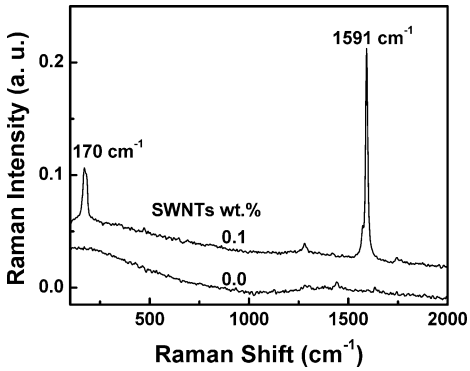

Figure 2. Raman spectra of pure nylon 6 and nylon 6−SWNT composite. The curves are labeled with the percentage of SWNTs in the polymer matrix.

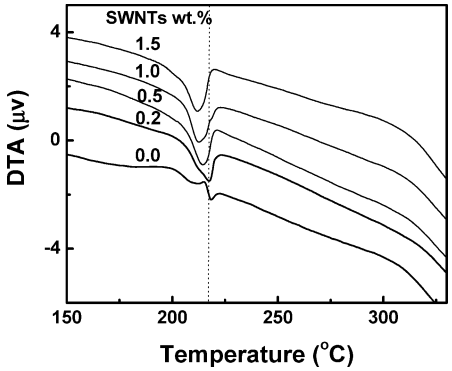

Figure 3. Differential thermal analysis (DTA) profiles of pure nylon 6 and nylon 6−SWNTs composites as a function of the SWNT loading.

During the composite synthesis the ring-opening polymerization of caprolactam proceeds mainly through the amine terminal group of PA6.[37−42] Condensation reactions between the carboxylic-acid groups of the SWNTs and the amino end group of PA6 terminate the chain propagation and result in the formation of lower molecular weight nylon (Scheme 1).[43] The introduction of a higher concentration of the carboxylic-acid-group-functionalized SWNTs into the reaction medium will consume more of the amino terminal groups of PA6 and thereby

(32) Liu, J.; Casavant, M. J.; Cox, M.; Walters, D. A.; Boul, P.; Lu, W.; Rimberg, A. J.; Smith, K. A.; Colbert, D. T.; Smalley, R. E. *Chem. Phys. Lett.* **1999**, *303*, 125−129.
(33) Ausman, K. D.; Piner, R.; Lourie, O.; Ruoff, R. S.; Korobov, M. *J. Phys. Chem. B* **2000**, *104*, 8911−8915.
(34) Niyogi, S.; Hamon, M. A.; Perea, D.; Kang, C. B.; Zhao, B.; Pal, S. K.; Wyant, A. E.; Itkis, M. E.; Haddon, R. C. *J. Phys. Chem. B* **2003**, *107*, 8799−8804.
(35) Zhao, B.; Itkis, M. E.; Niyogi, S.; Hu, H.; Zhang, J.; Haddon, R. C. *J. Phys. Chem. B* **2004**, *108*, 8136−8141.
(36) Zhao, B.; Itkis, M. E.; Niyogi, S.; Hu, H.; Perea, D.; Haddon, R. C. *J. Nanosci. Nanotechnol.* **2004**, *4*, 995−1004.
(37) Odian, G. *Principles of Polymerization*; Wiley: New York, 1991; Chapter 7.
(38) Kruissink, C. A.; Van der Want, G. M.; Staverman, A. J. *J. Polym. Sci.* **1958**, *30*, 67−88.
(39) Heikens, D.; Hermans, P. H.; Van der Want, G. M. *J. Polym. Sci.* **1958**, *30*, 81−104.
(40) Heikens, D.; Hermans, P. H.; Van der Want, G. M. *J. Polym. Sci.* **1960**, *44*, 437−448.
(41) Shalaby, S. W.; Reimschuessel, H. K. *J. Polym. Sci., Polym. Chem. Ed.* **1977**, *15*, 1349−1357.
(42) Stehlicek, J.; Sebenda, J. *Eur. Polym. J.* **1986**, *22*, 5−11.
(43) Zhang, Y.; Zhang, Q. L.; Cheng, K. L.; Xu, J. R. *J. Appl. Polym. Sci.* **2004**, *92*, 722−727.

Scheme 1. Synthesis of Nylon 6-SWNT Composite by Ring-Opening Polymerization of Caprolactam in the Presence of SWNTs

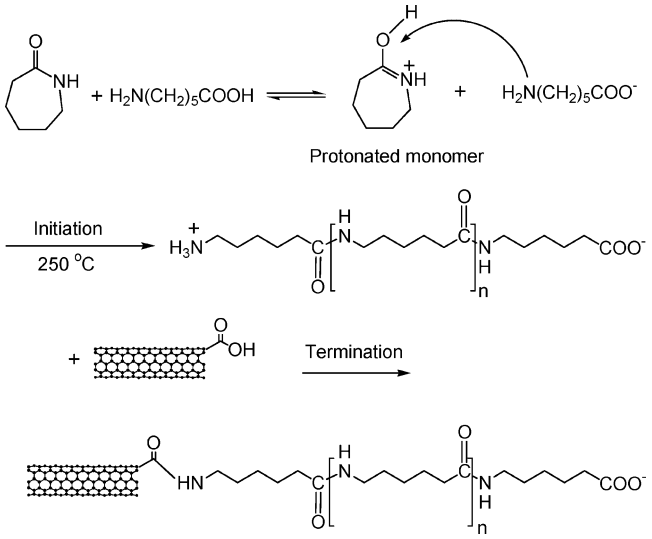

reduce the degree of polymerization and decrease the average molecular weight of the nylon 6.

2. Study and Characterization of the Nylon 6−SWNT Graft Copolymer. In the preceding section the incorporation of SWNTs in the composite was demonstrated by Raman spectra. However, this result does not confirm the covalent grafting of PA6 chains to the SWNTs, which is a primary goal of our processing procedure. To demonstrate the grafting copolymerization between SWNTs and PA6 chains and to estimate the grafting yield it is necessary to separate the SWNTs from the physically absorbed polymer chains.

As the weight ratio of 6-aminocaproic acid to caprolactam is about 10% in our experiments, a hard polymer composite with a very low fraction of SWNTs is expected. In this situation it is very difficult to separate the SWNTs from the polymer matrix. To separate the SWNTs from the nonchemically bonded PA6 we carried out a series of reactions with varying amounts of initiator using weight ratios of 6-aminocaproic acid to caprolactam of 0.0, 0.4, and 0.8 wt %. This decreased the polymerization rate and allowed us to study the effect of the initiator dose on the grafting yield. The experiments were performed for 6 h under identical conditions with a reaction temperature of 250 °C. The reaction products were washed with water to remove the unreacted monomer (caprolactam) and subsequently washed three times with formic acid to remove physically absorbed polymer. Due to the fact that the length of the SWNTs in the suspension (from ~0.5 to ~2 μm) is larger than the pore size of the filter paper (0.2 μm), most of the SWNTs are retained on the filter paper when this suspension is filtered. The native PA6 chains have high solubility in formic acid, and we therefore expect that only SWNTs and the PA6 chains which are grafted to SWNTs are left in the final product after the formic acid washing step.

If the 6-aminocaproic acid and the SWNTs are omitted from the reaction, the product does not show any precipitation in water, indicating the absence of the PA6 polymer. The addition of initiators allowed the observation of grafted PA6 chains on the SWNTs by IR spectroscopy (Figure 4). The broad band at 1640 cm^{-1} corresponds to the stretching vibration of the C═O

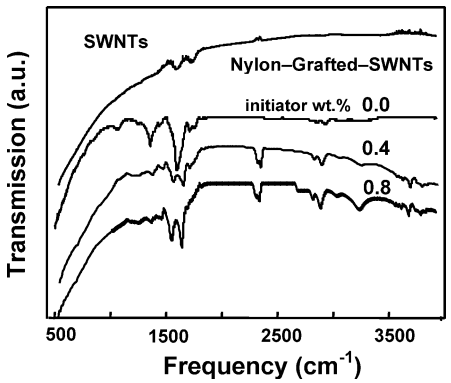

Figure 4. IR spectra of SWNTs with grafted nylon 6 (nylon-grafted-SWNTs) prepared using different initiator concentrations. The curves are labeled with the weight percentage of initiator concentration.

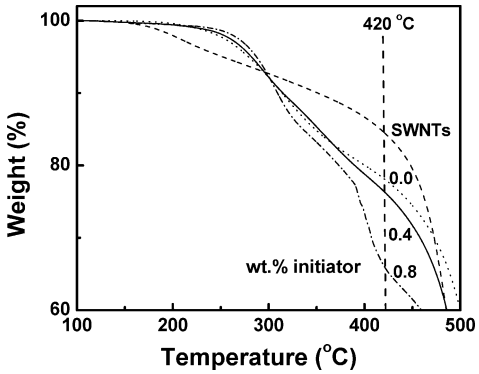

Figure 5. TGA of SWNTs and SWNTs with grafted nylon 6 prepared using different concentration initiators. The curves are labeled with the weight percentage of the initiator concentration.

group of the amide functionality.[44−46] The broad but slightly less intense band at 1540 cm^{-1} is assigned to a combination of the bending vibration of the N−H bond and the stretching vibration of the C−N bond of the amide group. The broad bands between 3000 and 3300 cm^{-1} are due to the hydrogen-bonded −COOH and −NH− groups of the PA6, whereas the C−H stretching vibrations occur at 2860 and 2930 cm^{-1}.[47] The IR results verify the existence of PA6 chains grafted to the SWNTs, irrespective of the presence of initiator in the reaction system. The relative intensity of the peaks in the 2800−3300 cm^{-1} region gradually increases with the initiator concentration, and this indicates that the presence of the initiator serves to increase the grafting yield of PA6 chains onto the SWNTs. This conclusion is further supported by the TGA data (Figure 5); the fraction of the sample decomposing below 420 °C, which is primarily composed of grafted PA6 chains, increases as the initiator concentration is increased. The grafting yield is approximately 25, 27, and 37 wt % at initiator concentrations of 0.0, 0.4, and 0.8 wt %, respectively. It should be noted that an initiator concentration of about 10 wt % of the reaction mixture is used in the composite synthetic procedure. Higher grafting yield than 37 wt % therefore should be expected in the final composite.

(44) Chen, J.; Hamon, M. A.; Hu, H.; Chen, Y.; Rao, A. M.; Eklund, P. C.; Haddon, R. C. *Science* **1998**, *282*, 95−98.
(45) Hamon, M. A.; Chen, J.; Hu, H.; Chen, Y.; Rao, A. M.; Eklund, P. C.; Haddon, R. C. *Adv. Mater.* **1999**, *11*, 834−840.
(46) Hu, H.; Zhao, B.; Hamon, M. A.; Kamaras, K.; Itkis, M. E.; Haddon, R. C. *J. Am. Chem. Soc.* **2003**, *125*, 14893−14900.
(47) Rodriguez-Rios, H.; Nuno-Donlucas, S. M.; Puig, J. E.; Gonzalez-Nunez, R.; Schulz, P. C. *J. Appl. Polym. Sci.* **2004**, *91*, 1736−1745.

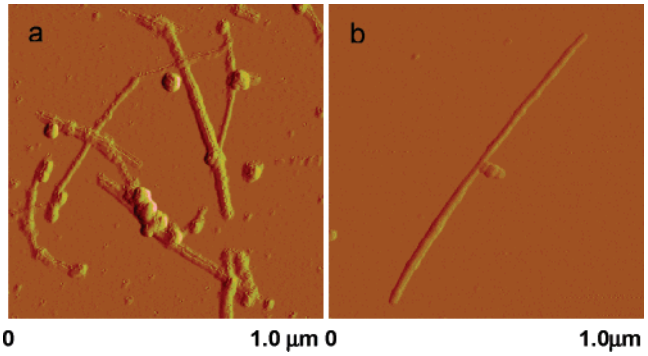

Figure 6. AFM images of (a) SWNTs with grafted nylon 6 prepared with 0.8 wt % initiator and (b) pristine SWNTs.

The SWNT solubility (or dispersability) changes after grafting polymerization, and this provides a clear indication that the PA6 chains are chemically bonded to the SWNTs and cannot be removed in the washing step. While pristine SWNTs cannot be well dispersed in formic acid (a good solvent for nylon 6), a very stable SWNT suspension can be formed in formic acid after the polymer grafting. This suggests that grafted PA6 chains are able to modify the properties of the SWNTs to the extent that the material becomes dispersible. AFM images of the soluble SWNTs show that their ends become thicker after grafting polymerization (Figure 6), as expected from a model in which the polymer chains are preferentially bonded to the open ends of the carbon nanotubes.[44,48]

The proposed mechanism for the grafting polymerization is illustrated in Scheme 1. The SWNTs used in the composite synthesis in this study are acid-treated nanotubes which contain approximately 3−4% carboxylic-acid sites.[30,48] The carboxylic-acid functionalities can react with the terminal amine group of PA6, and this leads to chain grafting of PA6 onto the SWNTs via the formation of an amide bond. This grafting polymerization reaction can only occur after 6-aminocaproic acid initiates the ring-opening polymerization of caprolactam, because carboxylic-acid groups themselves cannot initiate polymerization.[43] Assuming that each 6-aminocaproic acid initiates one ring-opening polymerization and leaves behind one reactive amine terminal group, higher 6-aminocaproic acid concentrations will generate more amine terminal groups in the reaction medium. This will increase the rate of condensation reactions between the carboxylic-acid groups of SWNTs and amine terminal groups of PA6 and thus facilitate the grafting polymerization. When the reaction was run in the absence of initiator, trace amounts of grafted oligomers were observed which we attribute to the presence of a small amount of water in the monomer that serves to initiate the ring-opening polymerization of caprolactam and the grafting reaction of PA6 chains with SWNTs.

As noted previously, in most composites the graphitic, atomically smooth surface of the SWNTs leads to a very weak interfacial interaction between the SWNTs and the polymer matrix. The approach adopted in the present work aims to exploit the presence of covalent linkages in the form of SWNT-grafted PA6 chains in order to overcome the weak interfacial adhesion.[49] In addition, based on the dissolution behavior it is apparent that the grafted polymer is also able to decrease the surface tension between the SWNTs and the polymer matrix, thereby increasing their compatibility.

3. Dispersion of SWNTs in Nylon 6 Matrix. The homogeneous dispersion of SWNTs in the polymer matrix is one of the most important requirements in achieving mechanical strength reinforcement because inhomogeneities can lead to structural defects in the composite material. Cross-sections of the composites were prepared by cutting the fibers in liquid nitrogen to give an intact surface fracture, and the resulting SEM images are shown in Figure 7.

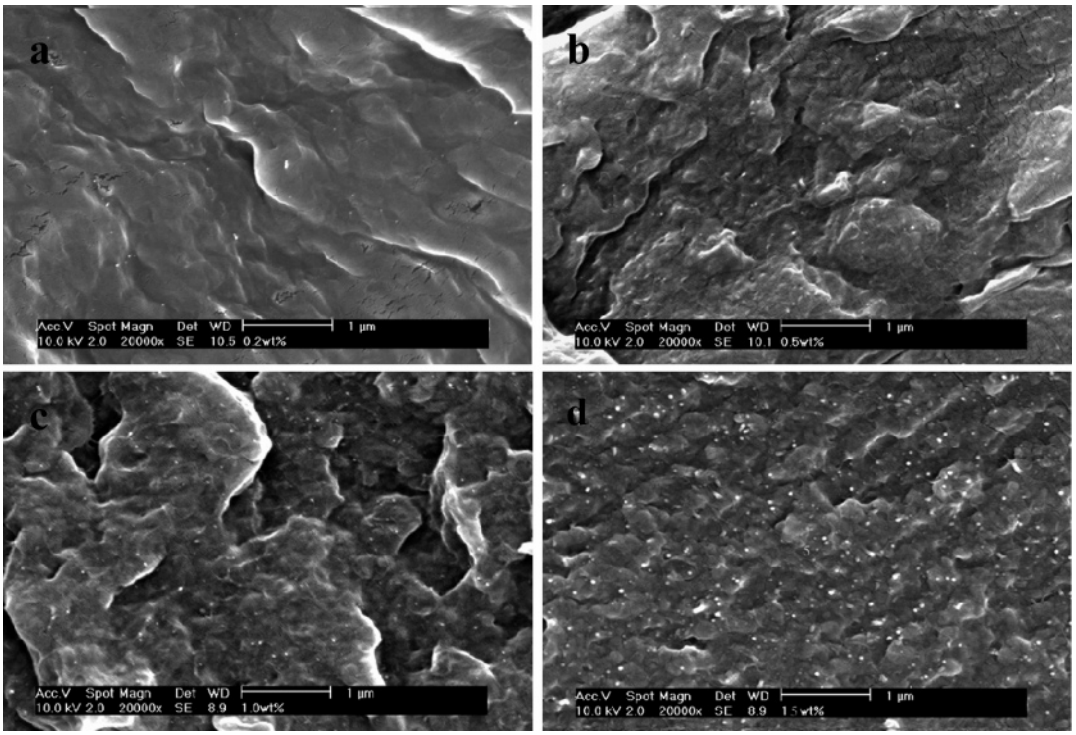

Figure 7. SEM images of the cross-sectional fracture of nylon 6−SWNTs composite fibers prepared with a SWNT loading of (a) 0.2, (b) 0.5, (c) 1.0, and (d) 1.5 wt %.

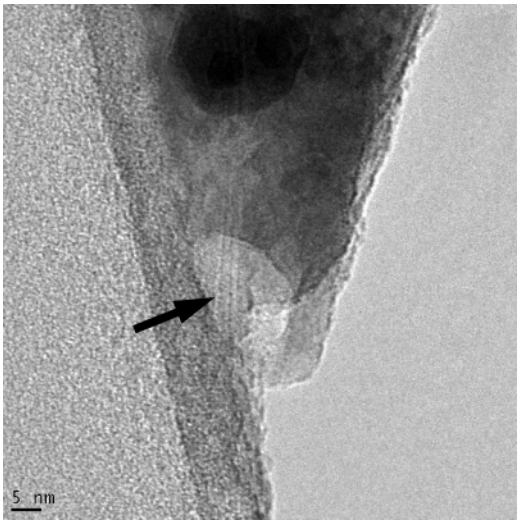

Figure 8. TEM image of nylon 6−SWNT composite fiber prepared with 0.2 wt % SWNT loading. The arrow shows a SWNT bundle incorporated in the polymer matrix.

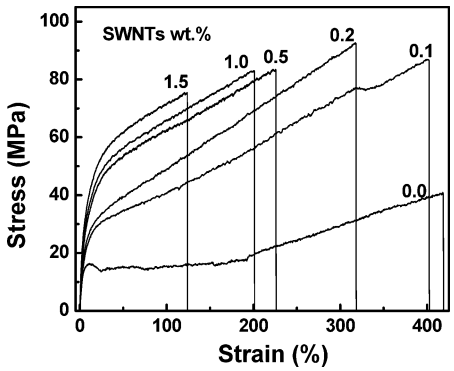

Figure 9. Stress−strain profiles of nylon 6−SWNT composite fibers at different SWNT loadings. The curves are labeled with the percentage of SWNTs in the polymer matrix.

The bright regions in these images are attributed to the SWNTs as a result of their high conductivity. It is apparent from Figure 7 that there are more bright regions in the composites with higher SWNT loading, and it is also evident that the SWNTs are homogeneously distributed in the nylon 6 matrix without aggregation. The typical diameter of the bright regions in the SEM images is approximately 20 nm. We believe that this is not the actual bundle size of SWNTs because the bright spot includes the SWNTs and the polymer that is closely associated with SWNTs. The TEM technique is able to penetrate the surrounding polymer and gives the SWNT texture in the composite; a typical bundle size for the SWNTs observed by TEM is approximately 5 nm as shown in Figure 8.

4. Mechanical Properties and Thermal Stability of Nylon 6 −SWNT Composite Fiber. To evaluate the effect of SWNT concentration on the properties of the reinforced composite, a range of nylon 6−SWNTs composite fibers was drawn by our melt processing technique with a spinneret exit diameter of $D_0 = 400\ \mu$m. The typical fiber diameter produced in our process is about 200 μm, and thus the draw ratio of the fibers is ∼4 (given by $(D_0/D)^2$, where D is the fiber diameter).

The mechanical properties were measured, and stress−strain profiles are illustrated in Figure 9. Pure nylon 6 shows a distinct yield point; the yield point is not observable for all the composites, probably due to the fact that the SWNTs are cross-linked with the nylon 6 matrix and this constrains the sliding of the PA6 chains. As prepared in our apparatus, pure nylon fiber shows a tensile strength of 40.9 MPa, which is approximately 130% higher than that of nylon film.[12] However the Young's modulus (440 MPa) of our fiber is only slightly higher than that of nylon film (396 MPa). The relatively low Young's modulus of the nylon fiber prepared in our spinneret is presumably due to the small draw ratio of the fiber. After the incorporation of SWNTs into the pure nylon, the Young's modulus and tensile strength of the composite fibers increase significantly, and the results are summarized in Table 1.

Table 1. Mechanical Properties of Nylon and Nylon 6−SWNT Composite Fibers

	pure nylon	0.1 wt % SWNTs	0.2 wt % SWNTs	0.5 wt % SWNTs	1.0 wt % SWNTs	1.5 wt % SWNTs
tensile strength (MPa)	40.9	86.0	92.7	83.4	83.0	75.1
Young's modulus (MPa)	440	540	657	840	1115	1200

Clearly, the incorporation of SWNTs into the nylon 6 matrix increases the tensile strength and Young's modulus, which indicates that the nylon fibers become tougher and more resistant to deformation. Directly mixing 1 wt % of SWNTs into the nylon 6 matrix[12] improved the Young's modulus and tensile strength of the composite by 456 and 22.3 MPa, respectively.[12] At the same carbon nanotube loading the nylon 6−SWNT composite prepared by our approach exhibits enhancements of 675 and 42.1 MPa in these parameters. However, the break strain (elongation at break), which is an indicator of the material flexibility, decreases with increasing nanotube loading. As shown in Figure 9, pure PA6 shows a break strain of 418%, while with 1.5 wt % SWNT loading, the break strain decreases to 122%. This implies that the presence of SWNTs serves to make the nylon 6 fiber stronger but less flexible.

It has been shown that SWNTs have extremely high thermal conductivity.[50,51] By improving the carbon nanotube−polymer interfacial interaction it is possible to impart the excellent thermal conductivity of SWNTs to the composite material, and it is known that the enhanced thermal conductivity of the composite can facilitate heat transport and thus increase its thermal stability.[52] We therefore investigated the thermal properties of the composites, and their DTA profiles are given in Figure 10. The temperature at the maximum mass loss rate in the DTA curve corresponds to the accepted thermal decomposition temperature of the composite. The results shown in Figure 10 indicate that composites with higher SWNT loading decompose at higher temperature, and this demonstrates that incorporation of SWNTs increases the thermal stability of the composite. In our experiments, the thermal decomposition temperature of pure nylon 6 is approximately 422 °C, and this value gradually increases as SWNTs are incorporated into the composite until the decomposition temperature reaches a value of 435 °C at a level of 1.5 wt % SWNTs.

(48) Hamon, M. A.; Hu, H.; Bhowmik, P.; Niyogi, S.; Zhao, B.; Itkis, M. E.; Haddon, R. C. *Chem. Phys. Lett.* **2001**, *347*, 8−12.
(49) Viswanathan, G.; Chakrapani, N.; Yang, H.; Wei, B.; Chung, H.; Cho, K.; Ryu, C. Y.; Ajayan, P. M. *J. Am. Chem. Soc.* **2003**, *125*, 9258−9259.
(50) Benedict, L. X.; Louie, S. G.; Cohen, M. L. *Solid State Commun.* **1996**, *100*, 177−180.
(51) Berber, S.; Kwon, Y. K.; Tomanek, D. *Phys. Rev. Lett.* **2000**, *84*, 4614−4616.
(52) Huxtable, S. T.; Cahill, D. G.; Shenogin, S.; Xue, L.; Ozisik, R.; Barone, P.; Usrey, M. L.; Strano, M. S.; Siddons, G.; Shim, M.; Keblinski, P. *Nat. Mater.* **2003**, *2*, 731−734.

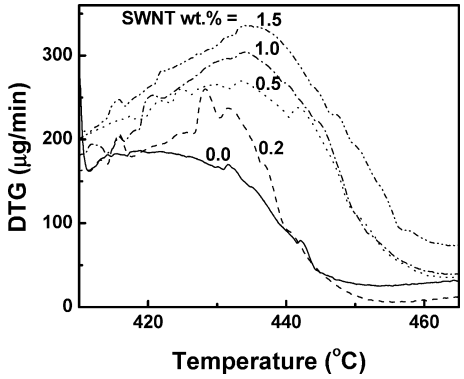

Figure 10. Thermal decomposition temperature of nylon 6−SWNTs composite at different SWNT loadings.

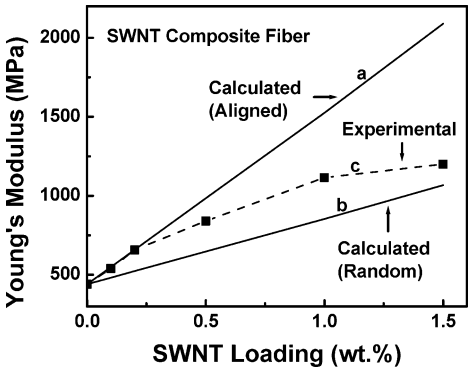

Figure 11. Young's modulus calculated from the Halpin−Tsai equation under the following assumptions: (a) SWNTs aligned along the axial direction of the fiber, (b) SWNTs randomly distributed as a 3D network within the fiber, and (c) experimental values of the Young's modulus.

5. Degree of SWNT Alignment in the Composite Fiber and Nature of the SWNT−Nylon 6 Interfacial Interaction. We carried out a rule-of-mixtures calculation to estimate the SWNT alignment and the nature of the SWNT−nylon 6 interfacial interaction within the composite fiber using densities of $\rho = 1500$ (SWNTs) and 1084 kg/m^3 (nylon 6). The average length, l, and diameter of the SWNT bundle, d, are taken to be $l = 1.0$ μm and $d = 5$ nm. For the Young's modulus (E_{NT}) and the tensile strength of the SWNT (σ_{NT}) we use $E_{NT} = 1$ TPa and $\sigma_{NT} = 22$ GPa. The Young's modulus of the composite was calculated under two assumptions: (a) SWNTs aligned along the axial direction of the fiber (Figure 11, curve a), (b) SWNTs randomly distributed as a 3D network within the fiber (Figure 11, curve b) using the Halpin−Tsai equations (see Supporting Information).[7,53,54] Figure 11 shows that the experimentally measured Young's modulus of the composite fiber (Figure 11, curve c) is very close to the theoretically predicted values under the assumption that the SWNTs are unidirectionally aligned within the fiber for SWNT loadings <0.5 wt %. The experimental data begin to deviate from curve a and shift toward curve b as the SWNT loading increases. This indicates that the SWNTs are aligned along the axial direction of the fiber, especially at low SWNT loading. However, the degree of alignment decreases as the SWNT loading increases, presumably due to the fact that the higher melting viscosity of the composite

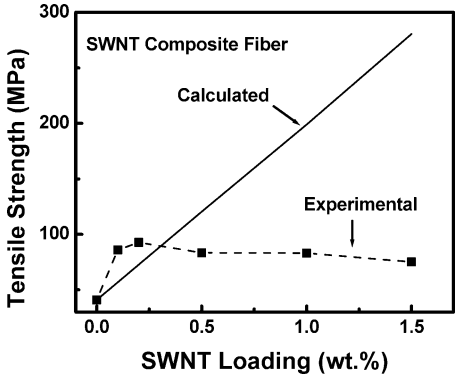

Figure 12. Tensile strength as a function of SWNT loading.

constrains the motion of the SWNTs in the matrix. We estimated the tensile strength from the equation $\sigma_c = \sigma_{NT}V_{NT} + \sigma_m V_m$,[55] where σ_c, σ_{NT}, and σ_m are the tensile strength of the composite, carbon nanotubes, and polymer matrix, respectively, and the results are summarized in Figure 12. It is evident that the experimentally measured tensile strength is higher than that of the theoretical estimate at low SWNT loadings and suggests that the interfacial interaction is very effective in strengthening the material when the SWNTs are aligned along the axial direction of the fiber. This behavior is to be expected and suggests that performance of the nylon 6-SWNT composite can be further improved by maintaining the SWNT alignment at higher loading.

Summary

We prepared nylon 6−SWNTs composite fibers by the in-situ ring-opening polymerization of caprolactam in the presence of SWNTs. The PA6 chains are found to be grafted to the SWNTs by a condensation reaction between the carboxylic-acid groups of the SWNTs and the terminal amino group of PA6. IR, TGA, and AFM results as well as SWNT solubility changes before and after grafting polymerization confirm the existence of grafted PA6 chains which are attached to the SWNTs. The grafting yield decreases with increasing initiator concentration. The grafted PA6 chains enhance the SWNT-nylon 6 interfacial interaction and improve their compatibility, and this allows a homogeneous dispersion of the SWNTs in the nylon matrix. The Young's modulus, tensile strength, and thermal stability of nylon 6 fibers are greatly improved by the incorporation of SWNTs via the current process, which may be readily scaled to manufacture nylon 6−SWNTs fibers in any length and quantity.

The novelty of our approach stems from the use of caprolactam to solvate the carbon nanotubes, which can then undergo in-situ polymerization to form the nanotube-nylon 6 composite. In this way we can exclude incidental solvents, and this precludes the possibility of SWNT aggregation in the composite which might be caused by evaporation of the solvent. Furthermore, our synthetic process promotes the chemical bonding of the PA 6 chains to the SWNTs, and this leads to the formation of a SWNTs−nylon hybrid materials which possess the characteristics of both SWNTs and nylon 6 and thereby enhances the interfacial interaction and the compatibility between the

(53) O'Regan, D. F.; Akay, M.; Meenan, B. *Compos. Sci. Technol.* **1999**, *59*, 419−427.
(54) Mallick, P. K. *Fibre-Reinforced Composites*; Marcel Dekker: New York, 1993.
(55) Agarwal, B. D.; Broutman, L. G. *Analysis and Performance of Fiber Composites*; Wiley: New York, 1980.

SWNTs and the polymer matrix. Our work represents a significant advance over previous studies in which SWNTs are first functionalized[23−27] or dispersed with the assistance of surfactant[18−22] and subsequently incorporated into a polymer matrix—the current procedure is a concise one-step process and is expected to dramatically reduce the synthetic cost of the composite.

Nylon 6 has played an important role in the field of engineering thermoplastics because of the combination of its excellent thermal and mechanical properties, broad processing range, and compatibility with additives and other materials; nylon 6 remains one of the most widely used polymer materials for fiber manufacturing.[56] The incorporation of 1.5 wt % SWNTs into nylon 6 increases the tensile modulus and tensile strength about 2.7 and 1.9 times, respectively. The dramatic improvement in the properties of this well-known material offers great promise for a number of areas where nylon 6 currently finds application.[57,58]

Acknowledgment. This research was supported by DOD/DARPA/DMEA under award no. DMEA90-02-2-0216. Carbon Solutions, Inc. acknowledges NSF SBIR Phase I and Phase II award nos. DMI-0110221 from the Division of Design, Manufacture and Industrial Innovation and a DARPA Phase I Award administered by the U.S. Army Aviation and Missile Command (award no. W31P4Q-04-C-R171). The authors are grateful to Dr. Erik T. Thostenson at the University of Delaware for his assistance in modeling the mechanical properties of the composite fibers.

Supporting Information Available: Photograph of continuous SWNT−nylon composite fiber about 200 meters in length, and description of the calculation of the Young's modulus and tensile strength. This material is available free of charge via the Internet at http://pubs.acs.org.

JA0446193

(56) Mark, H. F.; Kroschwitz, J. I. *Encyclopedia of polymer science and engineering*; Wiley: New York, 1988; Vol. 6.

(57) Ma, C. M.; Chang, F. *35th International SAMPE Symposium* **1990**, 59−72.

(58) Liou, W. J. *J. Reinf. Plast. Compos.* **1998**, *17*, 39−50.